



Picosecond difference-frequency-generation in orientation-patterned gallium phosphide

J. C. CASALS,^{1,5} S. PARSA,^{1,5} S. CHAITANYA KUMAR,^{1,2,*} K. DEVI,¹ P. G. SCHUNEMANN,³ AND M. EBRAHIM-ZADEH^{1,2,4}

¹ICFO-Institut de Ciències Fotoniques, Barcelona Institute of Science and Technology, 08860 Castelldefels (Barcelona), Spain

²Radiantis, Polígon Camí Ral, 08850 Gavà, Barcelona, Spain

³BAE Systems, Incorporated, MER15-1813, P.O. Box 868, Nashua, New Hampshire 03061-0868, USA

⁴Institució Catalana de Recerca i Estudis Avançats (ICREA), Passeig Lluís Companys 23, Barcelona 08010, Spain

⁵These authors contributed equally to this work.

*chaitanya.suddapalli@radiantis.com

Abstract: We report the generation of tunable high-repetition-rate picosecond radiation in the mid-infrared using the new quasi-phase-matched nonlinear material of orientation-patterned gallium phosphide (OP-GaP). The source is realized by single-pass difference-frequency-generation (DFG) between the output signal of a picosecond optical parametric oscillator (OPO) tunable across 1609–1637 nm with input pump pulses at 1064 nm in OP-GaP, resulting in tunable radiation across 3040–3132 nm. Using a 40-mm-long crystal, we have generated up to 57 mW of DFG average power at ~80 MHz repetition rate for a pump power of 5 W and signal power of 0.9 W, with >30 mW over >50% of the tuning range. The DFG source exhibits a passive power stability better than 3.2% rms over 1 hour in good spatial beam quality. To the best of our knowledge, this is the first picosecond frequency conversion source based on OP-GaP.

© 2017 Optical Society of America

OCIS codes: (190.4360) Nonlinear optics, devices; (190.7110) Ultrafast nonlinear optics; (190.4400) Nonlinear optics, materials; (190.4970) Parametric oscillators and amplifiers.

References and links

1. A. Tokmakoff, B. Sauter, and M. D. Fayer, "Temperature-dependent vibrational relaxation in polyatomic liquids: Picosecond infrared pump-probe experiments," *J. Chem. Phys.* **100**(12), 9035–9043 (1994).
2. M. Mathez, P. J. Rodrigo, P. Tidemand-Lichtenberg, and C. Pedersen, "Upconversion imaging using short-wave infrared picosecond pulses," *Opt. Lett.* **42**(3), 579–582 (2017).
3. M. Ebrahim-Zadeh and S. Chaitanya Kumar, "Yb-Fiber-laser-pumped ultrafast frequency conversion sources from the mid-infrared to the ultraviolet," *IEEE J. Sel. Top. Quant.* **20**(5), 624–642 (2014).
4. P. G. Schunemann, K. T. Zawilski, L. A. Pomeranz, D. J. Creeden, and P. A. Budni, "Advances in nonlinear optical crystals for mid-infrared coherent sources," *J. Opt. Soc. Am. B* **33**(11), D36–D43 (2016).
5. S. Chaitanya Kumar, P. G. Schunemann, K. T. Zawilski, and M. Ebrahim-Zadeh, "Advances in ultrafast optical parametric sources for the mid-infrared based on CdSiP₂," *J. Opt. Soc. Am. B* **33**(11), D44–D56 (2016).
6. S. Chaitanya Kumar, A. Agnesi, P. Dallochio, F. Pirzio, G. Reali, K. T. Zawilski, P. G. Schunemann, and M. Ebrahim-Zadeh, "Compact, 1.5 mJ, 450 MHz, CdSiP₂ picosecond optical parametric oscillator near 6.3 μm," *Opt. Lett.* **36**(16), 3236–3238 (2011).
7. S. Chaitanya Kumar, A. Esteban-Martin, A. Santana, K. T. Zawilski, P. G. Schunemann, and M. Ebrahim-Zadeh, "Pump-tuned deep-infrared femtosecond optical parametric oscillator across 6–7 μm based on CdSiP₂," *Opt. Lett.* **41**(14), 3355–3358 (2016).
8. L. Maidment, P. G. Schunemann, and D. T. Reid, "Molecular fingerprint-region spectroscopy from 5 to 12 μm using an orientation-patterned gallium phosphide optical parametric oscillator," *Opt. Lett.* **41**(18), 4261–4264 (2016).
9. P. G. Schunemann, L. A. Pomeranz, D. J. Magarrell, J. C. McCarthy, K. T. Zawilski, and D. E. Zelmon, "1064-nm-pumped mid-infrared optical parametric oscillator based on orientation-patterned gallium phosphide (OP-GaP)," in *Conference on Lasers and Electro-Optics (CLEO)* (Optical Society of America, 2015), paper SW30.4.
10. P. G. Schunemann, L. A. Pomeranz, and D. J. Magarrell, "First OPO based on orientation-patterned gallium phosphide (OP-GaP)," in *Conference on Lasers and Electro-Optics (CLEO)* (Optical Society of America, 2015), paper SW30.1.

11. J. Wei, S. Chaitanya Kumar, H. Ye, K. Devi, P. G. Schunemann, and M. Ebrahim-Zadeh, "Nanosecond difference-frequency generation in orientation-patterned gallium phosphide," *Opt. Lett.* **42**(11), 2193–2196 (2017).
12. S. Guha, J. O. Barnes, and P. G. Schunemann, "Mid-wave infrared generation by difference frequency mixing of continuous wave lasers in orientation-patterned Gallium Phosphide," *Opt. Mater. Express* **5**(12), 2911–2923 (2015).
13. G. Insero, C. Clivati, D. D'Ambrosio, P. Natale, G. Santambrogio, P. G. Schunemann, J. J. Zondy, and S. Borri, "Difference frequency generation in the mid-infrared with orientation-patterned gallium phosphide crystals," *Opt. Lett.* **41**(21), 5114–5117 (2016).
14. S. C. Kumar and M. Ebrahim-Zadeh, "High-power, fiber-laser-pumped, picosecond optical parametric oscillator based on MgO:sPPLT," *Opt. Express* **19**(27), 26660–26665 (2011).
15. L. A. Pomeranz, P. G. Schunemann, D. J. Magarrell, J. C. McCarthy, K. T. Zawilski, and D. E. Zelmon, "1- μ m-pumped OPO based on orientation-patterned GaP," *Proc. SPIE* **9347**, 93470K (2015).

1. Introduction

Tunable high-repetition-rate ultrafast sources in the mid-infrared (mid-IR) are of great interest for variety of applications, including pump-probe spectroscopy [1] and novel upconversion imaging techniques [2]. In the picosecond time-scale, such sources rely mainly on frequency down-conversion of widely available near-IR pump lasers in suitable nonlinear materials. While several quasi-phase-matched (QPM) nonlinear materials such as MgO-doped periodically-poled LiNbO₃ (MgO:PPLN), stoichiometric LiTaO₃ (MgO:sPPLT), and KTiOPO₄ (PPKTP) are readily available for mid-IR generation using the well-established pump laser technology near 1 μ m, the long wavelength transparency cut-off of these oxide-based crystals limits their mid-IR spectral coverage to \sim 4 μ m [3]. Alternative mid-IR nonlinear materials, such as AgGaSe₂ (AGSe), ZnGeP₂ (ZGP), CdSiP₂ (CSP) and orientation-patterned GaAs (OP-GaAs), can provide broadband spectral coverage deep into the mid-IR [4]. However, they require pumping beyond 2 μ m to avoid detrimental two-photon absorption at the pump wavelength. As such, significant efforts have been directed toward the development of novel mid-IR nonlinear materials with large bandgap that could offer wide transparency range and high nonlinearity, which could be deployed in combination with the mature, reliable, and widely available solid-state and Yb-fiber pump laser technology near 1 μ m, to enable wavelength generation beyond 4 μ m [5]. The recently developed birefringent nonlinear crystal, CdSiP₂ (CSP), is an excellent such example, providing spectral coverage across 6–8 μ m in the deep mid-IR when pumped at 1 μ m under noncritical phase-matching [6,7]. On the other hand, orientation-patterned gallium phosphide (OP-GaP) is a new QPM semiconductor nonlinear material with a wide transparency up to \sim 12 μ m, large optical nonlinearity ($d_{14} = 70.6$ pm/V) and high thermal conductivity (110 W/mK) [4]. Its large bandgap (2.26 eV) enables pumping at 1 μ m, making it a highly attractive alternative for the development of practical parametric sources throughout the mid- to deep-IR. In order to study the applicability of this new nonlinear material in its early stages of development for frequency conversion applications, it is important to evaluate the performance of the crystal in different spectral regions in the mid-IR and different time-scales to enable improvement in material quality to a suitable level for further development of efficient parametric sources into wavelength regions beyond \sim 4 μ m into the deep-IR.

Earlier reports on frequency conversion sources based on OP-GaP include a femtosecond optical parametric oscillator (OPO) synchronously pumped at 1040 nm, operating at 100 MHz, and providing spectral coverage in the 5–12 μ m wavelength range [8], a nanosecond doubly-resonant OPO (DRO) pumped at 1064 nm operating at 10 kHz [9], and a nanosecond DRO based on a 16.5-mm-long pumped at 2090 nm operating at 20 kHz [10]. Recently, we also demonstrated tunable difference-frequency-generation (DFG) in OP-GaP by mixing the input pulses from a nanosecond Nd:YAG laser and the signal from a MgO:PPLN OPO driven by the same laser at 80 kHz repetition rate [11]. In the continuous-wave (CW) regime, single-pass DFG based on OP-GaP using the pump wavelength of 1064 nm and signal wavelengths at 1550 nm [12] and 1301 nm [13] has also been reported.

Here, we report a high-repetition-rate, picosecond, single-pass DFG source based on OP-GaP, tunable over 92 nm in the mid-IR, across 3040-3132 nm. Using a 40-mm-long crystal, we have generated up to 57 mW of DFG power at 3042 nm at ~80 MHz repetition rate, with a passive power stability better than 3.2% rms over 1 hour. To the best of our knowledge, this is the first report on frequency conversion in OP-GaP in the picosecond time-scale.

2. Experimental setup

The schematic of the experimental setup for picosecond DFG in OP-GaP is shown in Fig. 1. The primary pump source is a mode-locked Yb-fiber laser (Fianium, FP1060-20) delivering up to 20 W of average power in ~20 ps pulses at ~80 MHz repetition rate. The pump laser operates at a central wavelength of 1064 nm with a full-width at half-maximum (FWHM) spectral bandwidth of 0.8 nm. A major portion of the output from the laser is used to synchronously pump a picosecond OPO [14] based on a 30-mm-long MgO:sPPLT nonlinear crystal with a grating period of $\Lambda = 30.65 \mu\text{m}$, providing temperature-tuned signal wavelengths from 1609 to 1637 nm in pulses of ~17 ps duration. The remaining power from the Yb-fiber laser is used as the pump for the DFG process. A variable delay line (DL) comprising mirrors, M_2 - M_5 , in the pump beam path enables synchronization of the pump and signal pulses for DFG in the OP-GaP crystal. The combination of a half-wave plate ($\lambda/2$) and polarizing beam-splitter (PBS) is used to adjust the pump power and a second half-wave plate is used to control the pump polarization for phase-matching in the crystal. A separate half-wave plate is used to control the signal polarization from the OPO. The pump and signal polarizations are independently optimized to achieve maximum DFG output power. Two converging lenses, L_1 ($f = 125 \text{ mm}$) and L_2 ($f = 50 \text{ mm}$), are used to adjust the diameter of the pump beam. The dichroic mirror, DM, which is coated for high reflection ($R > 99\%$) over 1300-2000 nm and high transmission ($T > 90\%$) at 1064 nm, is used to combine the pump and signal beams. The OP-GaP crystal used for DFG is a 40-mm-long sample with a single grating period of $\Lambda = 16 \mu\text{m}$. The crystal is 1.7-mm-thick and 6-mm-wide in aperture. However, we estimate the useful aperture of the crystal over which the QPM grating is available to be limited to $< 500 \mu\text{m}$. The crystal is housed in an oven which can be controlled from room temperature to 200°C with stability of $\pm 0.1^\circ\text{C}$. The 40-mm-long OP-GaP sample used for DFG in the mid-IR is shown in the inset of Fig. 1.

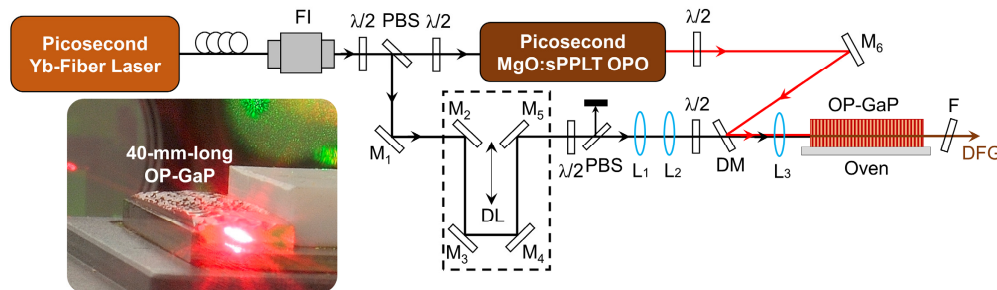


Fig. 1. Schematic of the experimental setup for the picosecond DFG in OP-GaP. FI: Faraday isolator, $\lambda/2$: Half-wave plate, PBS: Polarizing beam-splitter, Delay: variable delay line, L: Lens, M: Mirrors, F: Filter. Inset: The 40-mm-long OP-GaP crystal used for the DFG experiment, showing parasitic red light due to non-phase-matched sum-frequency-generation between the input pump and signal pulses.

The end-faces of the crystal are AR-coated ($R < 5\%$) at 1064 nm and 1500-1900 nm, with high transmission ($R < 25\%$) over 3000-3100 nm. Using a converging lens, L_3 ($f = 75 \text{ mm}$), the input beams are focused to a beam waist radius of $w_{0p} \sim 20 \mu\text{m}$ for the pump and $w_{0s} \sim 35 \mu\text{m}$ for the signal, corresponding to focusing parameters of $\xi_p \sim 5.4$ and $\xi_s \sim 2.77$, respectively. The DFG output beam in the mid-IR is filtered using a Ge long-pass filter (F).

3. Results and discussion

Initially, once the input beams were aligned through the OP-GaP crystal, we observed non-phase-matched sum-frequency-generation (SFG) between the pump and signal in the red part of the visible spectrum. We used this SFG signal to optimize the spatial overlap of the input beams as well as to find the suitable position in the OP-GaP crystal, by scanning position of the crystal in the horizontal and vertical directions. Although the crystal has a nominally large aperture of $1.7 \times 6 \text{ mm}^2$, we found only a few positions in the crystal that resulted in improved SFG output. At this point, with further increase in the input power, we observed DFG together with another SFG beam between the pump and the generated DFG again in the visible. The DFG signal was very sensitive to the position of the crystal. A small change in the crystal position resulted in a significant drop in the DFG power, indicating significant grating non-uniformity as well as a significantly smaller useful aperture than the nominal aperture over the 40-mm length of the OP-GaP crystal. Having finally established the conditions for the attainment of maximum DFG power, we then proceeded to characterize the picosecond DFG source by first investigating its wavelength tuning performance. This was achieved by simultaneously tuning the OPO signal wavelength from 1637 to 1609 nm and optimizing the phase-matching temperature of the OP-GaP crystal from 155°C to 192°C. The DFG temperature tuning results are presented in Fig. 2(a), where it can be seen that the source can be tuned over 92 nm in the mid-IR, from 3040 to 3132 nm. The experimental tuning data are in good agreement with the theoretical calculations using the relevant Sellmeier equations for OP-GaP [9]. The pump and signal wavelengths from the MgO:sPPLT OPO were measured using an infrared spectrum analyzer, while the DFG wavelength was inferred from energy conservation, and further confirmed by the parasitic SFG between the pump and the DFG output, measured using a visible spectrometer. While a maximum pump power of 15 W at 1064 nm was available for the experiments, up to 6 W was used to pump the MgO:sPPLT OPO, generating ~0.9 W of tunable signal output power. Further, we observed very low transmission through the 40-mm-long OP-GaP crystal at 1064 nm. Considering the low transmission, the pump power to DFG stage was limited to 5 W. Hence, we characterized the output power performance of the DFG source for a maximum pump power of 5 W at 1064 nm and a signal power of 0.9 W across the OPO wavelength range of 1637-1609 nm. The measured mid-IR average power across the tuning range of the picosecond DFG source is shown in Fig. 2(b). The average power varies from 57 mW at 3044 nm to 8.6 mW at 3132 nm, providing >30 mW over >50% of the tuning range. It is to be noted that the DFG powers presented here are not corrected for the AR-coating loss (~25%) of the OP-GaP crystal facets. Also shown in inset (i) of Fig. 2(b) is the pump spectrum centered at 1064 nm, with a FWHM bandwidth of ~0.8 nm. The measured OPO signal spectrum at 1636 nm, also exhibiting a FWHM spectral bandwidth of ~0.8 nm, is shown in the inset (ii) of Fig. 2(b). These spectral measurements were performed at maximum DFG power of 57 mW using a spectrum analyzer with ~0.1 nm resolution.

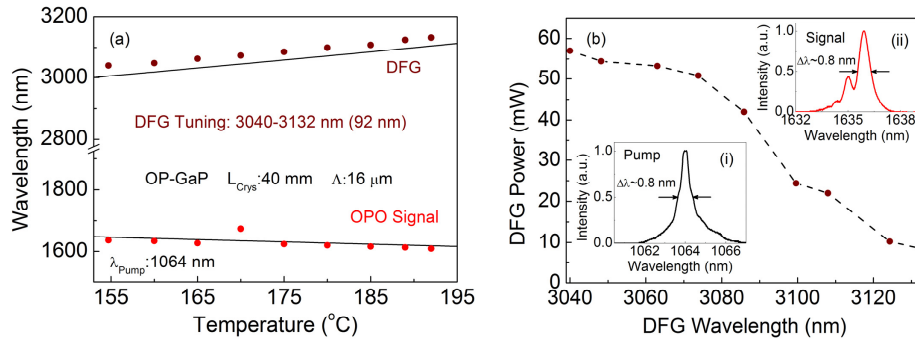


Fig. 2. (a) Temperature tuning performance of the picosecond DFG source based on OP-GaP. Solid and hollow circles represent the measured DFG and input signal wavelengths, and dashed lines are the theoretical calculations. (b) DFG output power across the tuning range. Inset: (i) pump, and (ii) signal spectra centered at 1064 nm and 1636 nm.

We then performed power scaling measurements of the DFG output as a function of the input pump and signal powers, with the results presented in Fig. 3(a) and 3(b). For a fixed signal power of 0.9 W, the DFG power scaling as a function of the input pump power is shown in Fig. 3(a). At each input pump power level, the phase-matching temperature was optimized to achieve maximum DFG power. As can be seen from the plot, we were able to generate as much as 57 mW of DFG average power at a phase-matching temperature of 153.5°C, for a maximum pump power of 5 W, at a slope efficiency of 1.7%. The corresponding phase-matching temperature was recorded to decrease from 167.5°C to 153.5°C. As the pump power was increased from 2 to 5 W, a significant temperature rise of ~14°C was observed in the OP-GaP crystal, which we attribute to absorption at the pump, signal and DFG wavelengths. In a separate experiment, we measured the transmission of OP-GaP crystal at the pump wavelength of 1064 nm at a temperature of 154.5°C, confirming a low transmission of ~52%. Considering the estimated losses at the pump and idler wavelengths, the measured DFG power of 57 mW corresponds to a single-pass conversion efficiency of ~4%/W. Although an absorption coefficient of 0.18 cm^{-1} has been reported in the literature [15], we were not able to measure such high transmission through our OP-GaP crystal. Moreover, the pump transmission was found to be inhomogeneous across the aperture of the crystal, and dependent on temperature as well as polarization of the incident beams. While the AR-coatings contribute to ~5% of the loss in the pump and signal wavelength range, our OP-GaP crystal exhibits unusually low transmission, which is expected to improve significantly with improvements in the crystal quality.

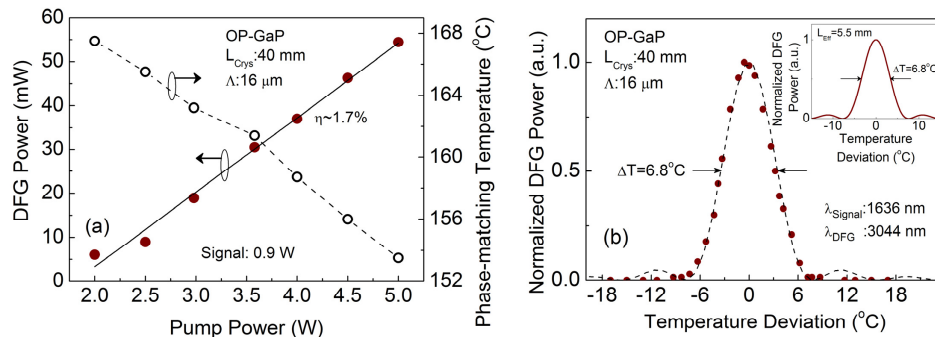


Fig. 3. DFG power scaling and OP-GaP phase-matching temperature as a function of the pump power at a fixed signal power, (b) Experimentally measured temperature acceptance bandwidth for DFG in the 40-mm-long OP-GaP crystal. Inset: Theoretically calculated DFG temperature acceptance bandwidth for an effective interaction length of 5.5 mm.

We also studied the temperature phase-matching acceptance bandwidth of the 40-mm-long OP-GaP crystal by measuring the DFG power as a function of crystal temperature, while operating at a signal wavelength of 1636 nm, and with the pump and signal power fixed at 2 W and 0.8 W, respectively. The normalized DFG power as a function of the temperature deviation about the measured phase-matching temperature of 167.5°C, is shown in Fig. 3(c). The dashed curve represents the sinc^2 fit to the experimental data, resulting in a FWHM temperature acceptance bandwidth of $\Delta T = 6.8^\circ\text{C}$. This is larger than the theoretically estimated bandwidth of $\Delta T = 0.9^\circ\text{C}$ for a 40-mm-long OP-GaP crystal using the Sellmeier equations for the material [9]. On the other hand, using the experimentally measured temperature acceptance bandwidth, we estimated an effective interaction length of ~ 5.5 mm, as shown in the inset of Fig. 3(c). The discrepancy between the calculated and experimental acceptance bandwidth values could be attributed to imperfections in the uniformity and duty-cycle errors of the QPM grating period over the full 40-mm length of the OP-GaP sample, resulting in a useful interaction length substantially shorter than the actual physical length. We also calculated the spectral acceptance bandwidth for the 40-mm-long crystal to evaluate its impact on conversion efficiency and output power using the relevant Sellmeier equations [9]. For a fixed input OPO signal wavelength at ~ 1635 nm, we obtained a FWHM spectral acceptance bandwidth of ~ 0.1 nm for the pump at ~ 1064 nm. This is significantly smaller than the FWHM bandwidth of the Yb-fiber pump laser (~ 0.8 nm), thus significantly limiting conversion efficiency and output power in the present experiment. Other factors relate to the confinement and non-uniformities in the useful aperture of the crystal along its 40-mm length, which result in non-optimum overlap of the pump and signal beam along the propagation direction over the full crystal length, similarly leading lower nonlinear conversion efficiency and reduced effective interaction length.

We further recorded the long-term stability of the DFG output power together with the pump and signal, with the results shown in Fig. 4(a) and 4(c). The measurements were performed at a DFG wavelength of 3044 nm, for a pump power of 5.2 W and an input signal power of ~ 0.7 W at 1636 nm. As can be seen from Fig. 4(a) and 4(b), the pump and signal exhibit a passive power stability better than 0.2% rms and 2.4% rms, respectively, over 1 hour, while the DFG output, shown in Fig. 4(c), has a stability better than 3.2% rms over 1 hour, with a mean DFG power of 53 mW. For the attainment of maximum nonlinear frequency conversion efficiency, it is crucial to achieve optimum temporal overlap between the interacting input beams. While the temporal overlap is achieved by perfect synchronization of the pump and signal pulses using

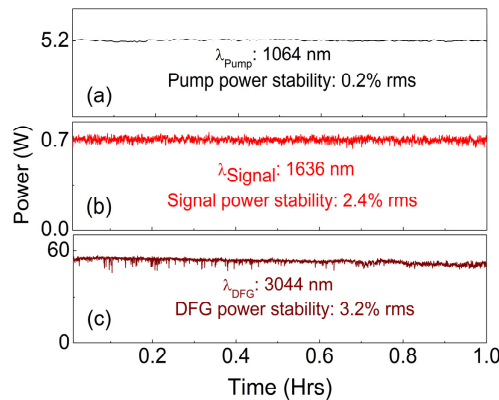


Fig. 4. Long-term power stability of the (a) pump at 1064 nm, (b) signal at 1636 nm, and (c) DFG at 3044 nm recorded over 1 hour.

the delay line (see Fig. 1), the group velocity mismatch (GVM) between the pump and signal determine the effective temporal walk-off length. The GVM between the pump and signal

pulses calculated using the relevant Sellmeier equation and thermos-optic coefficients [9], as a function of signal wavelength is shown in Fig. 5(a), where it can be seen that the GVM varies from ~ 591 - 593 fs/mm in the signal wavelength range of interest. For the minimum pulse duration of 17 ps, this corresponds to an effective temporal interaction length ~ 29 mm. We then investigated the effect of temporal synchronization on the DFG output. The variation of the normalized DFG power as a function of the time delay between the two pulses is shown in Fig. 5(b). As can be seen, the measured time delay has a FWHM of $\Delta\tau \sim 10$ ps, consistent with the pump and signal pulse durations of ~ 20 ps and ~ 17 ps, respectively.

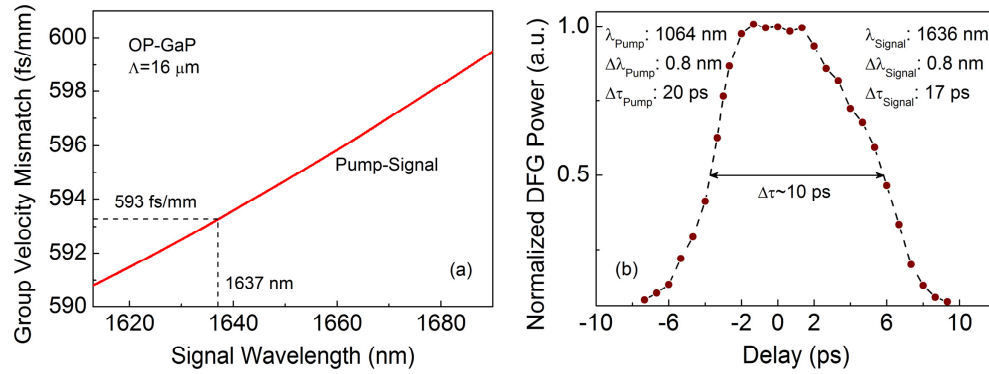


Fig. 5. Group velocity mismatch between the pump and signal pulses in the OP-GaP crystal (b) Normalized DFG power as a function of the pump delay.

The far-field energy distribution of the input pump and signal beams at 1064 nm and 1636 nm, and the generated mid-IR DFG beam at 3044 nm, were recorded using a pyroelectric camera, and are presented in Fig. 6(a) and 6(c). The results confirm that the generated DFG beam exhibits TEM_{00} spatial profile with single-peak Gaussian distribution and a circularity of $\sim 73\%$. In spite of the fact that the pump and signal beams exhibit circularity of $>95\%$, the ellipticity in the DFG output indicates the spatial confinement of generation to the lower part of beam due to the tapering of the QPM grating resulting in non-ideal grating period and duty-cycle errors over the 40-mm length of the OP-GaP crystal.

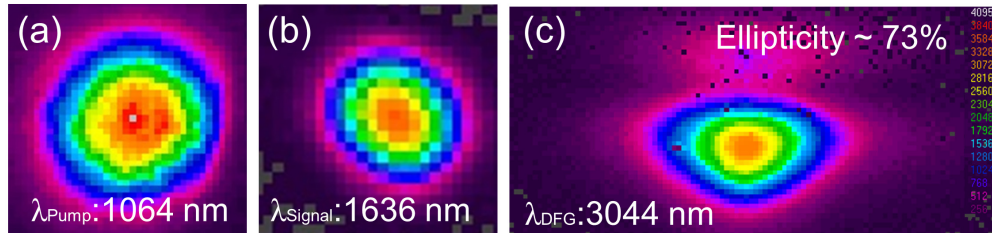


Fig. 6. Spatial beam profiles of the (a) pump at 1064 nm, (b) signal at 1636 nm, and (c) DFG at 3044 nm.

4. Conclusions

In conclusion, we have demonstrated what we believe to be the first picosecond frequency conversion source based on OP-GaP crystal, providing practical powers and wavelength tuning in the mid-IR at a high repetition rate of ~ 80 MHz. The source is based on single-pass DFG of a mode-locked Yb-fiber laser at 1064 nm and tunable signal pulses from a picosecond MgO:PPsLT OPO synchronously pumped by the same laser. The generated radiation is tunable across 3040-3132 nm in the mid-IR, providing up to 57 mW of average power, with >30 mW over $>50\%$ of the tuning range, for an input pump power of 5 W and signal power of ~ 0.9 W, in TEM_{00} spatial beam quality with a circularity of $\sim 73\%$. The

temperature phase-matching acceptance measurements have resulted in a FWHM bandwidth of $\Delta T = 6.8^\circ\text{C}$, corresponding to an effective interaction length of 5.5 mm, substantially shorter than the physical crystal length of 40 mm. The generated DFG beam at 3044 nm exhibits a passive power stability better than 3.2% rms over 1 hour. We have also studied the effect of temporal overlap between the input pump and signal beams using the variable delay line for synchronization of the two pulse trains for the attainment of maximum DFG efficiency and output power. The generated average power and conversion efficiency are currently limited by the spectral acceptance bandwidth of the 40-mm-long OP-GaP crystal for the pump. Other factors include non-optimal uniformity and duty cycle errors of the QPM grating, as well as the confined and non-uniform useful aperture along the full crystal length, as implied by the short effective interaction length of 5.5 mm obtained from the measurement of temperature acceptance bandwidth of the 40-mm-long crystal. These point to the feasibility of enhanced output power and efficiency using OP-GaP crystals with improved overall optical quality, grating uniformity and useful aperture over shorter interaction lengths, enabling practical realization of high-repetition-rate picosecond sources in the mid-IR. Given the increased tolerance in the fabrication of QPM gratings for DFG and parametric generation at longer wavelengths, due to the larger required grating periods ($\Lambda \sim 19\text{-}36$ for $\lambda \sim 4\text{-}12\ \mu\text{m}$), the prospects for the development of efficient high-average-power picosecond sources further into the deep-IR based on OP-GaP appear even more encouraging. Our first demonstration of a high-repetition-rate picosecond DFG source in the mid-IR is an important first step in this direction.

Funding

Ministerio de Economía y Competitividad (MINECO) (nuOPO, TEC2015-68234-R); European Commission (Project Mid-Tech, H2020-MSCA-ITN-2014); CERCA Programme / Generalitat de Catalunya, Severo Ochoa Programme for Centres of Excellence in Research and Development (SEV-2015-0522); Fundació Privada Cellex.